CHEMICAL ENGINEERING TRANSACTIONS
VOL. 95, 2022
A publication of AIDIC
The Italian Association of Chemical Engineering
Online at www.cetjournal.it
Guest Editors: Selena Sironi, Laura Capelli

ISBN 978-88-95608-94-5; **ISSN** 2283-9216
DOI: 10.3303/CET2295048

Characterization of Quartz Sand as an Adsorbent for Anionic Surfactant Adsorption with Presences of Alkaline and Polymer

Tengku Amran, Tengku Mohd[a,b]*, Nur Amelina Bohairah[a], Mohd Zaidi Jaafar[b]

[a]School of Chemical Engineering, College of Engineering, Universiti Teknologi MARA, 40450 Shah Alam, Selangor, Malaysia
[b]School of Chemical and Energy Engineering, Faculty of Engineering, Universiti Teknologi Malaysia, 81310 Johor Bahru, Johor, Malaysia
amran865@uitm.edu.my

Alkaline-surfactant-polymer (ASP) flooding is a formulation designed on the basis of alkali, surfactant and polymer flooding to enhance oil recovery, however, surfactant loss in ASP could degrade the efficiency of the process. This study highlights the characterization of quartz sand as an adsorbent for adsorption of anionic Sodium Dodecyl Sulphate (SDS) surfactant with presences of alkaline and polymer. Quartz sand was characterized using SEM-EDX and FTIR analyses. For static adsorption tests, three systems were formulated, namely Surfactant, Alkaline-Surfactant (AS) and Alkaline-Surfactant-Polymer (ASP), respectively. 10,000 ppm sodium carbonate (Na_2CO_3) and 500 ppm of anionic Hydrolyzed Polyacrylamide (HPAM) polymer were formulated with varying surfactant concentration, which were mixed with the quartz sand at a fixed mass-to-volume ratio of 1:5. Under SEM-EDX analysis, quartz sand analysed as grain with relief and crescentic marks and SiK was found as the highest mineral component with 43.48%. FTIR results have found the spectrums representing SDS surfactant at specific peaks after treatment of quartz sand, which confirmed that surfactant adsorption has occurred. The equilibrium adsorption results showed that the highest surfactant adsorption was obtained by surfactant formulation (0.93 mg/g), while the lowest adsorption was exhibited by ASP (0.34 mg/g), a significant reduction of 63% with presences of alkaline and polymer in the formulation.

1. Introduction

Alkaline-surfactant-polymer (ASP) flooding has been developed on the basis of alkaline flooding, surfactant flooding and recognized as one of the most economical techniques for chemical enhanced oil recovery (cEOR) (Olajire, 2014). The effectiveness of this method depends on the selection of the appropriate alkaline, surfactant and polymer and how they are mixed to achieve a compatible formulation. Synergistic reaction between alkaline and surfactant results in ultra-low IFT, while polymer contributes by enhancing the viscosity of the aqueous phase to create more favourable mobility ratio (Mohd et al., 2018), leading to better displacement and sweep efficiency, which greatly improve the oil recovery. However, ASP flooding has potential disadvantages of forming scaling deposition, precipitation, and loss of chemical solutions on the surface of reservoir formation (Owusu and Asumadu-sarkodie, 2016). During ASP flooding, chemical solutions such as polymer and surfactant tend to adsorb on the surface of sandstone formation. High surfactant adsorption affects the ASP to be economically unfeasible due to the expensive cost of surfactant (Pal et al., 2018). Therefore, it is crucial to design a chemical solution that effectively reduce the amount of chemical adsorption and incorporate an effective monitoring method during such recovery processes. Mohd et al. (2017) has reviewed and suggested a real-time approach of streaming potential measurement using electrodes permanently installed downhole to monitor the efficiency of ASP flooding. Several studies have discussed the effect of surfactant concentration on the adsorption of ionic surfactant onto reservoir formation. Anionic surfactants are the most common type of surfactant in sandstone formation because it results in reduction of excessive adsorption due to the repulsive force between the negatively surface charged of formation and the anionic head group (Belhaj et al., 2020). Most of the EOR processes fail due to unknown characteristics of explored reservoir rocks, as Saha et al. (2018) stated that surfactant adsorption behaviour

Paper Received: 15 June2022; Revised: 10 August 2022; Accepted: 30 September 2022
Please cite this article as: Amran T., Mohd T., Bohairah T.A., Jaafar M.Z., 2022, Characterization of Quartz Sand as an Adsorbent for Anionic Surfactant Adsorption with Presences of Alkaline and Polymer, Chemical Engineering Transactions, 95, 283-288 DOI:10.3303/CET2295048

strongly influenced by the surface area of rock and its charge species associated with the fluid interface. Quartz sand (SiO_2), also known as silica sand, is commonly chosen to investigate the water-silica system because of its high abundancy and crystalline silica phase stability (Mohd and Jaafar, 2019). The quartz sand composition strongly influences the ionic surfactant adsorption between solid and liquid interface, resulting in a negative charge on the sand surface. Therefore, this research is conducted to characterize the quartz sand and evaluate the surfactant adsorption in ASP formulation, while aiming to minimise surfactant adsorption. Yet, there are still uncertainties regarding the surfactant adsorption behaviour with presences of alkaline and polymer. Additionally, the characteristics and purity of quartz sand used are not well known and understood, necessitating further characterisation analysis to be conducted. The outcomes of this study may result in a decline in surfactant adsorption on quartz sand surface when ASP solution is used instead of surfactant solution alone.

2. Methodology

2.1 Materials

Three types of chemicals were used in this laboratory work, namely surfactant, alkaline and polymer. Anionic Sodium Dodecyl Sulphate (SDS) with 99% purity was obtained from Merck. Sodium Carbonate (Na_2CO_3) was chosen for alkaline obtained from QREC while partially hydrolyzed polyarylamide (HPAM) polymer was purchased from VChem, China. All chemicals were used as received without further purification. Selection of those chemicals are based on the most common and widely used in EOR applications. The quartz sand used as adsorbent was obtained from the sea sand at Pantai Port Dickson, Malaysia, which was sieved at the desired range of 125-200 µm with further purification.

2.2 SEM and EDX Analysis

The adsorbent firstly was purified numerous times with distilled water. Quartz sand was immersed for 12 hours in a strong hydrochloric acid solution and then clean within 5 minutes in 0.1M NaOH to remove impurities. The quartz sand was rinsed with water and dried at 110^{o}C to remove any remaining acid. The size and structure of the adsorbent was determined using scanning electron microscopy (SEM), while the component minerals were determined using energy dispersive x-ray spectroscopy (EDX). A dried quartz sand sample was coated with gold, and about 10nm of conductive layer was to improve picture quality and eliminates the charging effect.

2.3 Fourier Transform Infrared (FTIR) Spectroscopy Analysis

PerkinElmer Spectrum-2 FTIR spectrophotometer was utilized to examine the adsorbent particles or structure before and after ASP flooding. The adsorbent's molecular structure was acquired in the range of 400 to 4000 cm^{-1}. To prepare the standard sample, 5 mg of adsorbent sample (after being dried) was thoroughly mixed with potassium bromide (KBr). Top plate and hole were cleaned using acetone before starting the analysis. The sample was dried to remove any moisture content, before being inserted into the hole and purge it. This study analyzed quartz sand before and after surfactant treatment, and the pattern of spectrum was observed referring to infrared spectroscopy (IR) adsorption table to identify functional groups present in the sample.

2.4 Static adsorption tests

Static adsorption test for anionic surfactants was conducted using 4g of quartz sand in 20 mL of surfactant solution. surfactant solution was prepared at different concentration from 150 ppm to 2000 ppm. In static adsorption study, there were three systems formulated, namely surfactant, AS and ASP. For surfactant formulation, the mixture of sand and surfactant solution was agitated on a shaker controller for 24 hr at room temperature. Then, the mixtures were centrifuged at 3000 rpm for 30 mins to effectively separate the solid and the solutions. After that, the supernatant solution was filtered and transferred into a 20 mL centrifuge tube for further UV-Visible analysis to obtain the equilibrium concentration. The sand samples were dried at 120 °C for 24 hr and transferred into glass bottle for further FTIR study. The same exact method was employed for AS in the presence of 10,000 ppm sodium carbonate and ASP in the presence of 10,000 ppm sodium carbonate and 500 ppm HPAM polymer, respectively. The adsorption of surfactant was determined from calibration curve constructed from different surfactant concentrations. A graph of an absorbance against surfactant concentration was used to determine the surfactant concentration after adsorptions from the peak wavelength. A suitable wavelength value is determined by selecting the wavelength which provides a higher absorbance value. For SDS surfactant, the UV-Vis spectrophotometer was set at 264 nm as it provides higher absorbance value. Then, a graph of an absorbance against concentration of surfactant is plotted. The procedure was repeated with a range of various different concentration samples. The adsorption rate is then calculated using Equation 1.

$$q = \frac{V}{M}(C_o - C_e) \quad (1)$$

Where q is adsorption capacity (mg/g), V is the volume of surfactant solution (L), M is the weight of quartz sand (g) and C_o and C_e is the initial and equilibrium concentration (mg/L).

3. Results and discussion

3.1 SEM and EDX Analysis

The SEM images of quartz sand was observed under scale bar of 10µm, 50µm and 100µm as shown in Figure 1a, 1b and 1c, respectively, whereby the size, shape and structure were further analyzed. In the scale bar of 100µm, most shape detected was cuboid shape with feature of subangular grain with edge rounding. The image of quartz sand full of sharp edge from every subangular, which can be furthered analyzed as grain with relief. When observing the image under scale bar of 10µm and 50µm, crescentic marks can be seen indicates of specific element present as composition in the adsorbent (Helland et al., 1997). Adsorption process can be enhanced through porous surface which came from irregular shape and size of pores, which the rough surface enlarges the surface area of quartz sand particles, thereby increase the adsorption capacity (Kalińska-Nartiša et al., 2017). From the EDX analysis shown in Figure 2, few elements were traced, specifically with the weight percentage. The SiK element gives the highest weight%, which is 43.48%, followed by O K, FeL, MnK and AlK with 42.68%, 7.24%, 5.60% and 1.01%, respectively. Quartz sand employed in this study might be asserted to contain mesoporous silica, which comprised of irregular and asymmetrical particle sizes (Sheng et al., 2018).

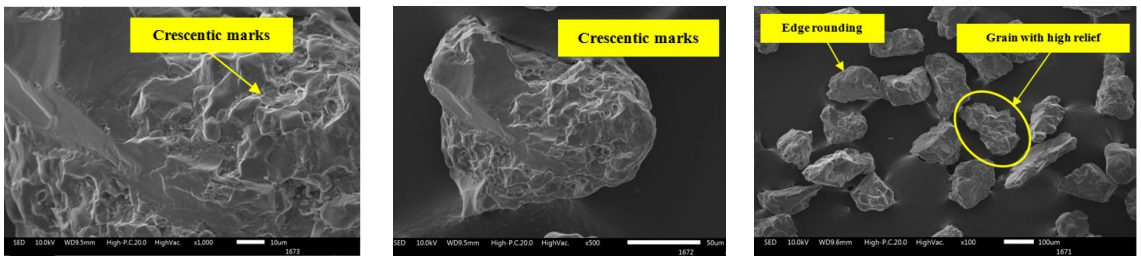

(a) (b) (c)

Figure 1: SEM imagery in quartz surface (a) crescentic marks in 10 µm; (b) crescentic marks in 50 µm; (c) edge rounding and grain with high relief in 100 µm.

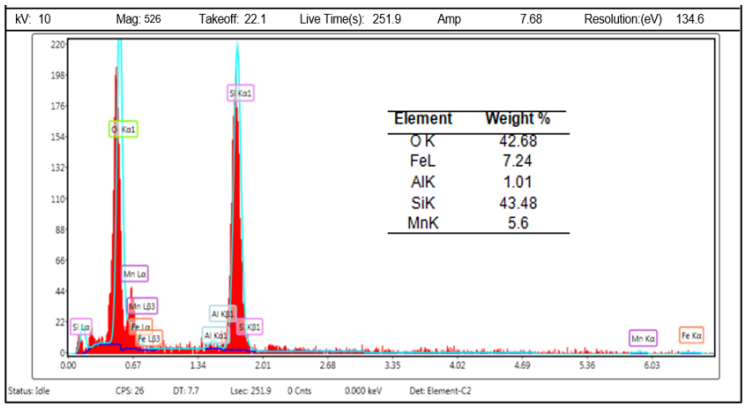

Figure 2: EDX analysis of quartz sand

3.2 FTIR analysis

The FTIR spectra of the quartz sand samples were collected from 4000 to 400 cm^{-1}. FTIR analysis has been extensively applied to the identification and classification of minerals. The functional group of quartz sand was determined by absorption frequency spectra. The absorbance spectrums were recorded after scanning on the FTIR for pure sand prior to adsorption. The FTIR spectrum of pure quartz sand and after being treated with surfactant, AS and ASP at 2000 ppm surfactant concentration is shown in Figure 3. Figure 3a illustrates the FTIR spectrum for pure quartz sand as the control sample. The absorption bands appearing at 523 cm^{-1}, 695.34 cm^{-1}, and 777.32 cm^{-1} suggested the presence of quartz mineral as the main composition in the sand particles (Ramasamy et al., 2009). While the peak of the infrared spectra was at 1738.08 cm^{-1}, which is in the

region of Si-O symmetric representing the C=O stretch bending vibration. The FTIR spectrum of quartz sand after being treated with surfactant is shown as in Figure 3b. The peaks at 778 cm^{-1}, 693 cm^{-1} and 523 cm^{-1} are related to the Si-O-Si bonding and stretching vibration of the quartz group (Ramasamy et al., 2009). The stretching vibrational mode at 1381 cm^{-1} comes from the sulfonate group (S=O), which can be assigned to the bending of the aldehyde from SDS group. The observed spectrum at 2920 cm^{-1} and 2858 cm^{-1} were assigned to CH_2 asymmetric stretching vibration of SO_2 molecule resulting from the packing of SDS group (Bera et al., 2013). This spectrum indicates the adsorption of SDS occurred on the surface of the sand after being treated with surfactant. Additionally, the wavenumbers of the S=O signals decreased from 1080.5 cm^{-1} to 1072.0 cm^{-1}, a change that was resulted from the chemical adsorption on quartz (Chen et al., 2019). The FTIR spectrum of quartz sand after being treated with AS is illustrated in Figure 3c. The spectrum showed that some characteristic of adsorption bands of SDS have shifted from 2920 cm^{-1} to 2925 cm^{-1} (Gong et al., 2015) and from 1381 cm^{-1} to 1384 cm^{-1} (Bera et al., 2013). The absorption peak appeared at approximately 2854 cm^{-1} was due to the stretching vibrations of CH_2 in SDS group (Chen et al., 2019). The characteristic adsorption bands of sodium carbonate appeared at 871 cm^{-1}, 712 cm^{-1}, 1687 cm^{-1} and 1427 cm^{-1} belong to the stretching vibrations of C=O bonds in the carbonate ion from sodium carbonate (Ren et al., 2014). These results proved that sodium carbonate interfered with the adsorption of SDS on the quartz surface. A stretching vibration band of S=O at 1076.1 cm^{-1} was due to the interaction between the solid and the chemical solutions (Alharthi et al., 2020), indicating that SDS was chemically adsorbed on the quartz surface. Figure 3d illustrates the FTIR spectrum of quartz sand after being treated with ASP. The spectrum showed that some characteristic adsorption bands of SDS disappeared and some characteristic adsorption bands of sodium carbonate and HPAM polymer have appeared. The bands at 1450 cm^{-1}, 874 cm^{-1}, 711 cm^{-1} belong to the stretching vibrations of C=O bonds in carbonate anion from alkaline. The spectrums at 1718 cm^{-1} and 1656 cm^{-1} referred to the C=O stretching vibration which were assigned for the presence of aldehyde in HPAM polymer (Hospodarova et al., 2018). The weak band appeared at 1350 cm^{-1} referred to the alkyl C-H stretch from SDS group, which indicated that SDS was adsorbed on the sand surface. These spectrums showed that surfactant and polymer were bound on the surface of the quartz sand. However, the scope of this study was limited to surfactant adsorption without specific quantitative measurement of polymer adsorption.

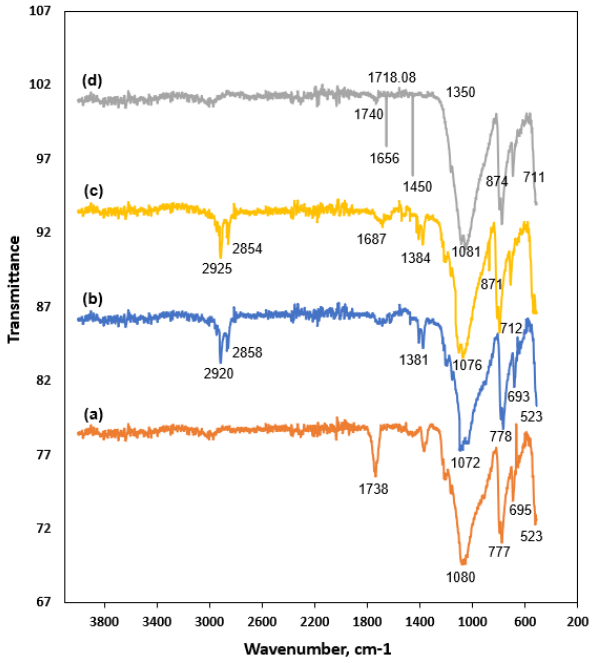

Figure 3: FTIR spectra of quartz sand particles before and after adsorption: a) pure sand; b) after surfactant treatment; c) after AS treatment; d) after ASP treatment.

3.3 Surfactant Adsorption

Figure 4 illustrates the surfactant adsorption on quartz sand at different surfactant concentration with and without the presences of alkaline and polymer. From the figure, it is shown that adsorption of anionic surfactant increases with increasing surfactant concentration due to the formation of hemi-micelles. SDS surfactant is adsorbed by quartz due to the capability of the formation mineral to generate a variable charge

(Azam et al., 2013). At low surfactant concentration, adsorption takes place because of the electrostatic interaction between the electrically charge head group of the surfactant and the charges present on the quartz surface. Higher surfactant concentration increases the number of surfactant molecules per unit volume, resulting in increase of surfactant adsorption onto the rock surface (Dang et al., 2011). Sharp increase of surfactant adsorption is observed as it reaches 1000 ppm due to the aggregation of surface colloids including hemi–micelles and admicelles between hydrocarbon chain and the surface monomer. As the surfactant concentration increases to 2000 ppm, the adsorption rate gradually increases because the surface charge is electrically neutralized by the adsorbed surfactant ion (Ramanaiah et al., 2016). At higher surfactant concentration, the adsorption occurred due to the aggregation of the surfactant monomer by hydrophobic interaction (Kwok et al., 1995). Above CMC, plateau phase is reached, which indicates additional concentration added to the system keeps the surfactant adsorption to be constant as most of the active sites are adsorbed with surfactant and micelles are repelled by the adsorbed surfactant molecule (Elias et al., 2016). Figure 5 illustrates the significant reduction of surfactant adsorption with addition of alkaline and polymer into the formulation obtained at 2000 ppm surfactant concentration. Individual surfactant formulation exhibited maximum adsorption of 0.93 mg/g, followed by AS and ASP with amount of adsorbed surfactant of 0.57 mg/g and 0.34 mg/g, respectively. A significant reduction of approximate 63% was observed from surfactant formulation to ASP when incorporating alkaline and polymer with surfactant solution. The effectiveness of ASP system on quartz sandstone proved that synergistic of alkaline, surfactant and polymer can greatly minimize adsorption of anionic surfactant (Sheng, 2011).

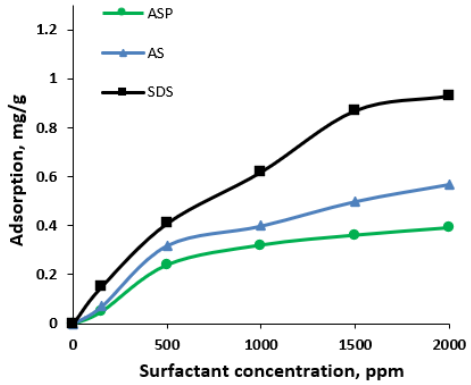

Figure 4: Surfactant adsorption at different surfactant concentration with alkaline and polymer formulation

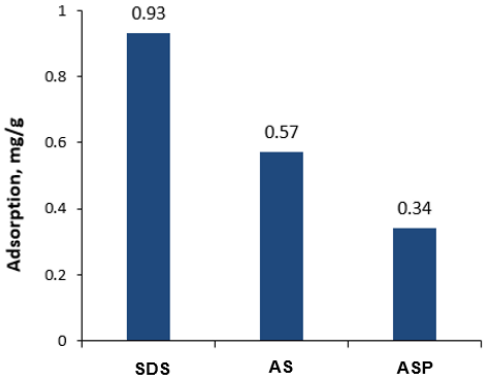

Figure 5: Reduction of surfactant adsorption for different systems formulated at 2000 ppm

4. Conclusion

The characterization of quartz sand by FTIR analysis found the spectrums representing SDS surfactant and HPAM polymer appeared at specific peaks after the treatment of quartz sand. These spectrums have confirmed that surfactant and polymer were attached on the surface of the quartz sand through adsorption. However, only surfactant adsorption has been observed in this research without quantifying the polymer adsorption in the formulation. Under SEM-EDX analysis, quartz sand was analysed as grain with relief and crescentic marks, while SiK detected with 43.48% as the highest mineral component. The static adsorption tests were conducted in the presence and absence of alkaline and polymer in the surfactant formulation, which discovered favourable adsorption reduction of anionic surfactant with presences of alkaline and polymer. Reduction of surfactant adsorption was driven by the electrostatic interaction between the negative surface charges of the quartz and the negative SDS ions with presence of sacrificial agent. Presences of alkaline and polymer as the ASP formulation exhibited the lowest adsorption with approximately 63% reduction from surfactant formulation at 2000 ppm surfactant concentration. Therefore, the incorporation of anionic surfactant with alkaline and polymer in a system provides significant and synergistic impact in minimizing the adsorption of anionic surfactant on the quartz sand.

Acknowledgments

The authors would like to thank the School of Chemical Engineering, College of Engineering, Universiti Teknologi MARA for the facilities and support provided. This research work was financially supported by the Geran Penyelidikan Khas (GPK) (600-RMC/GPK 5/3 (189/2020)) granted by Universiti Teknologi MARA (UiTM).

References

Alharthi, S.S., Alzahrani, A., Ali, M.A.N., Mohammed, B., 2020, Spectroscopic and Electrical Properties of Ag_2S/PVA Nanocomposite Films for Visible-Light Optoelectronic Devices, Journal of Inorganic and Organometallic Polymers and Materials, 30, 3878–3885.

Azam, M.R., Tan, I.M., Ismail, L., Mushtaq, M., Nadeem, M., Sagir, M., 2013, Static adsorption of anionic surfactant onto crushed Berea sandstone, Journal of Petroleum Exploration and Production Technology, 3, 195–201.

Belhaj, A.F., Elraies, K.A., Mahmood, S.M., Zulkifli, N.N., Akbari, S., Hussien, O.S.E., 2020, The effect of surfactant concentration, salinity, temperature, and pH on surfactant adsorption for chemical enhanced oil recovery: a review, Journal of Petroleum Exploration and Production Technology, 10(1), 125–137.

Bera, A., Kumar, T., Ojha, K., Mandal, A., 2013, Adsorption of surfactants on sand surface in enhanced oil recovery: Isotherms, kinetics and thermodynamic studies, Applied Surface Science, 284, 87–99.

Chen, X., Gu, G., Liu, D., Zhu, R., 2019, The flotation separation of barite-calcite using sodium silicate as depressant in the presence of sodium dodecyl sulfate, Physicochemical Problems of Mineral Processing, 55(2), 346-355.

Dang, C.T.Q., Chen, Z., Nguyen, N.T.B., Bae, W., Phung, T.H., 2011, Development of isotherm polymer/surfactant adsorption models in chemical flooding. SPE Asia Pacific Oil & Gas Conference and Exhibition, Jakarta, Indonesia.

Elias, S., Rabiu, A., Oyekola, O., Seima, B., 2016, Adsorption characteristics of surfactants on different petroleum reservoir materials, The Online Journal of Science and Technology, 6(4), 6–16.

Gong, W., Zang, Y., Xie, H., Liu, B., Chen, H., Li, C., Ge, L., 2015, Properties of surfactants on high salt-affected sandy land in enhanced sand fixation: Salt tolerance, adsorption isotherms and ecological effect, RSC Advances, 5, 81847-81856.

Helland, P.E., Huang, P.H., Diffendal, R.F.,1997, SEM analysis of quartz sand grain surface textures indicates alluvial/colluvial origin of the quaternary “glacial” boulder clays at Huangshan (Yellow Mountain), east-central China, Quaternary Research, 48(2), 177–186.

Hospodarova, V., Singovszka, E., Stevulova, N., 2018, Characterization of Cellulosic Fibers by FTIR Spectroscopy for Their Further Implementation to Building Materials, American Journal of Analytical Chemistry, 9, 303-310.

Kalińska-Nartiša, E., Lamsters, K., Karušs, J., Krievans, M., Rečs, A., Meija, R., 2017, Quartz grain features in modern glacial and proglacial environments: A microscopic study from the Russell Glacier, southwest Greenland, Polish Polar Research, 38(3), 265–289. https://doi.org/10.1515/popore-2017-0018

Mohd, T.A.T., Jaafar, M.Z., 2019, Adsorption of anionic sodium dodecyl sulfate surfactant on local sand and kaolinite surfaces: The prospect of Alkaline and Salinity, International Journal of Recent Technology and Engineering, 7(6), 972–979.

Mohd, T.A.T., Jaafar, M.Z., Rasol, A.A.A., Ali, J., 2017, A new prospect of streaming potential measurement in alkaline-surfactant polymer flooding, Chemical Engineering Transactions, 56, 1183–1188.

Mohd, T.A.T., Taib, N.M., Adzmi, A.F., Ab Lah, N.K.I.N., Sauki, A., Jaafar, M.Z., 2018, Evaluation of polymer properties for potential selection in enhanced oil recovery, Chemical Engineering Transactions, 65, 343-348.

Olajire, A.A., 2014, Review of ASP EOR (alkaline surfactant polymer enhanced oil recovery) technology in the petroleum industry: Prospects and challenges, Energy, 77, 963–982.

Owusu, P.A., Asumadu-sarkodie, S., 2016, A review of renewable energy sources, sustainability issues and climate change mitigation, Civil & Environmental Engineering Review Article, 1–14.

Ramanaiah, M., Gouthamsri, S., Balakrishna, M., Ramaraju, B., Nageswara Rao, G., 2016, Effect of anionic micelles of sodium dodecyl sulfate on protonation equilibria of salicylic acid derivatives, Cogent Chemistry, 2(1), 1217762.

Ramasamy, V., Rajkumar, P., Ponnusamy, V., 2009, Depth wise analysis of recently excavated Vellar river sediments through FTIR and XRD studies, Indian Journal of Physics, 83(9), 1295–1308.

Ren, F., Ding, Y., Leng, Y., 2014, Infrared spectroscopic characterization of carbonated apatite: A combined experimental and computational study, Journal of Biomedical Materials Research Part A, 102(2), 496-505.

Saha, R., Uppaluri, R.V.S., Tiwari, P., 2018, Effect of mineralogy on the adsorption characteristics of surfactant—Reservoir rock system, Colloids and Surfaces A: Physicochemical and Engineering Aspects, 531, 121–132.

Sheng, J.J., 2011, Surfactant Flooding, Modern Chemical Enhanced Oil Recovery: Theory and Practice.

Sheng, L., Zhang, Y., Tang, F., Liu, S., 2018, Mesoporous/microporous silica materials: Preparation from natural sands and highly efficient fixed-bed adsorption of methylene blue in wastewater, Microporous and Mesoporous Materials, 257, 9–18.